

Magnetic properties of FeSe superconductor

G.E. Grechnev,^{1,*} A.S. Panfilov,¹ V.A. Desnenko,¹ A.V. Fedorchenko,¹
S.L. Gnatchenko,¹ D.A. Chareev,² O.S. Volkova,³ and A.N. Vasiliev³

¹*B. Verkin Institute for Low Temperature Physics and Engineering,
National Academy of Sciences of Ukraine, 61103 Kharkov, Ukraine*

²*Institute of Experimental Mineralogy, Russian Academy of Sciences,
Chernogolovka, Moscow Region 142432, Russia*

³*Department of Low Temperature Physics, Moscow State University, Moscow 119991, Russia*

A detailed magnetization study for the novel FeSe superconductor is carried out to investigate the behavior of the intrinsic magnetic susceptibility χ in the normal state with temperature and under hydrostatic pressure. The temperature dependencies of χ and its anisotropy $\Delta\chi = \chi_{\parallel} - \chi_{\perp}$ are measured for FeSe single crystals in the temperature range 4.2 – 300 K, and a substantial growth of susceptibility with temperature is revealed. The observed anisotropy $\Delta\chi$ is very large and comparable with the averaged susceptibility at low temperatures. For a polycrystalline sample of FeSe, a significant pressure effect on χ is determined to be essentially dependent on temperature. *Ab initio* calculations of the pressure dependent electronic structure and magnetic susceptibility indicate that FeSe is close to magnetic instability with dominating enhanced spin paramagnetism. The calculated paramagnetic susceptibility exhibits a strong dependence on the unit cell volume and especially on the height Z of chalcogen species from the Fe plane. The change of Z under pressure determines a large positive pressure effect on χ which is observed at low temperatures. It is shown that the literature experimental data on the strong and nonmonotonic pressure dependence of the superconducting transition temperature in FeSe correlate qualitatively with calculated behavior of the density of electronic states at the Fermi level.

PACS numbers: 74.70.Xa, 74.62.Fj, 75.10.Lp, 75.30.Cr

I. INTRODUCTION

Soon after the discovery of superconductivity in LaFeAsO_{1-x}F_y, the superconductivity was also detected in the binary compound FeSe_{1-x}¹ with transition temperature $T_c \simeq 8$ K. This compound possesses the simplest crystal structure among the new families of Fe-based superconductors, and consists of a stack of Fe square planar layers, which are tetrahedrally coordinated by Se atoms. Also the large pressure effect on transition temperature was later observed²⁻⁴ with $T_c \approx 37$ K at pressures $P \approx 9$ GPa, indicating that FeSe_{1-x} is actually a high temperature superconductor. Therefore, the superconducting FeSe_{1-x} compound has attracted considerable attention and is a subject of intensive studies for the last years⁵⁻¹². The structural simplicity of FeSe favors experimental and theoretical studies of chemical substitution and high pressure effects, which are aimed at promoting a better understanding of a mechanism of the superconductivity.

Upon cooling below room temperature, the tetragonal $P4/nmm$ phase of FeSe_{1-x} undergoes a subtle distortion to the lower symmetry orthorhombic $Cmma$ phase^{3,5-7}. This transition occurs within a broad temperature range, about 70÷100 K, depending on the stoichiometry of the samples. It was also found that the tetragonal phase undergoes structural transitions under high pressures ($P \geq 10$ GPa) to the hexagonal non-superconducting $P6_3mmc$ NiAs-type phase^{2,3,5}, and then to its orthorhombic modification ($Pbnm$, MnP-type)^{2,13,14}. The recent theoretical examination of stability regions of the high pres-

sure phases of FeSe_{1-x}^{15,16} indicated a possibility of metallization and superconductivity in the orthorhombic $Pbnm$ phase under high pressure.

Though a substantial increase of T_c was clearly observed under pressure^{2,3,17-19}, these studies did not detect any magnetic ordering. However, recent NMR studies provided some indication of an incipient magnetic phase transition under pressure²⁰. Recently, a static magnetic ordering has been detected above $P \sim 1$ GPa by means of zero-field muon spin rotation (ZF μ SR)^{21,22} and neutron diffraction²². These studies have revealed that as soon as magnetic ordering emerges, the magnetic and superconducting states apparently coexist, and both the magnetic ordering temperature T_N and T_c increase simultaneously with increasing pressure. Also, it was recently found, that upon applying pressure the increase of T_c in FeSe_{1-x} appeared to be nonmonotonic and exhibits a local maximum at $P \simeq 0.8$ GPa, which is followed by a local minimum at $P \sim 1.2$ GPa^{17,18,21,22}. Therefore, there is still a considerable controversy regarding an interplay between electronic structure, magnetism and superconductivity in the FeSe_{1-x} compound, especially under pressure.

The experimental data on magnetic susceptibility of FeSe_{1-x} system in the normal state are incomplete and contradicting^{8,12}. Also, these data are mostly obtained on polycrystalline samples and often distorted by the presence of secondary magnetic phases of iron. In order to shed more light on the relation between magnetic and superconducting properties, it is very important to elucidate the intrinsic susceptibility of FeSe_{1-x} supercon-

ductors and investigate its evolution with doping, temperature, and pressure. Here we report on results of the experimental studies of magnetic properties for single-crystalline and polycrystalline FeSe samples of high quality in the normal state. These studies include measurements of the temperature dependence of magnetic susceptibility and its anisotropy as well as the hydrostatic pressure effects. The experimental investigations are supplemented by *ab initio* calculations of the electronic structure and magnetic susceptibility of FeSe. The calculations are based on the local-spin-density approximation (LSDA) of the density-functional theory (DFT). The results of experiments and calculations are used to analyze the nature of magnetism in FeSe and the basic mechanisms of its strong pressure dependence.

II. EXPERIMENTAL DETAILS AND RESULTS

The plate-like single crystals of FeSe_{1-x} superconductor were grown in evacuated quartz ampoules using the KCl/AlCl₃ flux technique with a constant temperature gradient of 5° C per cm along the ampoule length (temperature of the hot end was kept at 427° C, temperature of the cold end was about 380° C). Typical dimensions of the produced single crystalline samples are (2÷3)×(2÷3)×(0.3÷0.5) mm³. The tetragonal *P4/nmm* structure was demonstrated at room temperature by X-ray diffraction technique. The energy dispersive X-ray spectroscopy, performed on a CAMECA SX100 (15 keV) analytical scanning electron microscope, revealed Fe:Se=1:0.96±0.02 composition denoted in the following as FeSe for simplicity.

The study of magnetic properties of FeSe samples at ambient pressure was carried out at $T = 4.2 \div 300$ K by using a SQUID magnetometer. The superconducting transition was detected within 6÷8 K. The magnetization dependencies $M(H)$ in magnetic fields up to 5 T appeared to be close to linear, indicating that the concentrations of ferromagnetic impurities are negligibly small. A typical temperature dependence of the magnetic susceptibility for single crystalline FeSe samples is shown in Fig. 1. As is seen, a substantial growth of susceptibility with temperature was revealed in the normal state, as well as a large magnetic anisotropy.

The study of magnetic susceptibility of FeSe under helium gas pressure P up to 0.2 GPa was performed at fixed temperatures 78 and 300 K by using a pendulum-type magnetometer placed directly in the nonmagnetic pressure cell²³. In order to measure the pressure effect with a reasonable accuracy, a sufficiently large mass of the sample is required. We have used the FeSe sample, further called as "polycrystalline" FeSe, which was prepared by compacting a number of about 50 of small arbitrarily oriented single crystals inside of an aluminum foil cylinder. The total mass of the sample was about 200 mg. The measurements were carried out in the field $H = 1.7$ T and their relative errors did not exceed 0.5%. The exper-

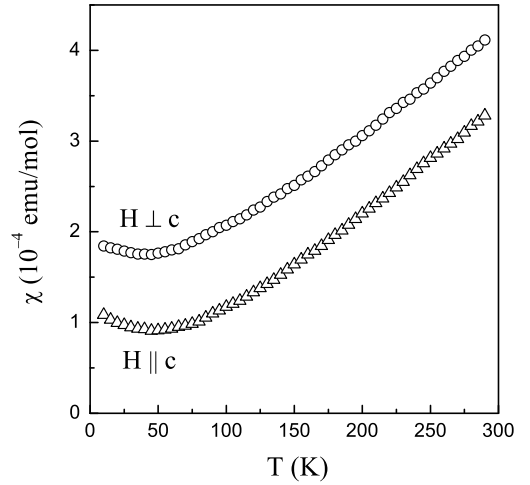


FIG. 1: Temperature dependence of the magnetic susceptibility in the normal state for the single-crystalline FeSe measured in the field $H = 50$ mT. Data corresponding to the magnetic field directions $H \perp c$ axis and $H \parallel c$ are denoted by \circ and \triangle symbols, respectively.

imental pressure dependencies $\chi(P)$ at different temperatures are shown in Fig. 2, which demonstrates their linear character. The negative value of the pressure effect, $d \ln \chi / dP \simeq -6.5 \times 10^{-2} \text{ GPa}^{-1}$, was observed at temperature 300 K, whereas at $T = 78$ K the effect appeared to be positive, $d \ln \chi / dP \simeq 10 \times 10^{-2} \text{ GPa}^{-1}$. The available experimental and theoretical results on $d \ln \chi / dP$ for FeSe are compiled in Table I together with corresponding data for the relative FeTe compound for comparison.

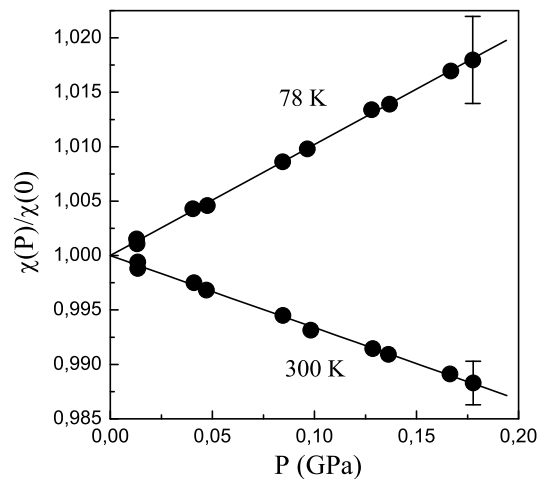


FIG. 2: Pressure dependencies of the magnetic susceptibility, normalized to its value at $P = 0$, for the polycrystalline FeSe compound at temperatures 78 and 300 K. The solid lines are guides for the eye.

TABLE I: Pressure derivatives of the magnetic susceptibility $d\ln\chi/dP$ (in units 10^{-2} GPa^{-1}) for FeSe and FeTe compounds at different temperatures.

	$T(\text{K})$	$d\ln\chi/dP$	
		FeSe	FeTe ^b
experiment:	300	-6.5 ± 1	13 ± 1
		~ -7 ^a	
	78	10 ± 3	23 ± 1.5
		~ 6.5 ^a	
	20	~ 9 ^a	
theory:	0	$\simeq 8$	~ 20

^a From NMR Knight shift data of Ref. 20

^b Results for FeTe are taken from Ref. 24

III. COMPUTATIONAL DETAILS AND RESULTS

In order to analyze the magnetic properties of FeSe compound in the normal state, the *ab initio* calculations of the electronic structure and paramagnetic susceptibility were carried out. At ambient conditions FeSe compound possesses the tetragonal PbO-type crystal structure (space group $P4/nmm$), which is composed by alternating triple-layer slabs. Each iron layer is sandwiched between two nearest-neighbor layers of Se, which form edge-shared tetrahedra around the iron sites. The positions of selenium layers are fixed by the structural parameter Z , which represents the relative height of Se atoms above the iron plane. The structural parameters of FeSe were determined by means of X-ray and neutron diffraction^{3,6,7,9,14,25}.

The main purpose of the present *ab initio* calculations was to evaluate the paramagnetic response in an external magnetic field and to elucidate the nature and features of magnetism in the normal state of FeSe compound. In the context of this task, the dependencies of the magnetic susceptibility on volume, lattice parameters and temperature were addressed. *Ab initio* calculations of the electronic structure of FeSe were performed by employing a full-potential all-electron relativistic linear muffin-tin orbital method (FP-LMTO, code RSPt^{26,27}). The exchange-correlation potential was treated within the local spin density approximation²⁸ of the DFT. The calculated basic features of electronic structure of FeSe appeared to be in a qualitative agreement with results of previous DFT calculations²⁹⁻³².

As is seen in Figs. 3 and 4, the calculated band structure and density of electronic states (DOS) of FeSe indicate the presence of the hybridized predominantly *d*-like Fe electronic states close to the Fermi level E_F . The chalcogen *p*-states are situated well below E_F and slightly hybridized with the *d*-states of iron. Also, one can see a van Hove singularity in Fig. 4 at $\sim 40 \text{ meV}$

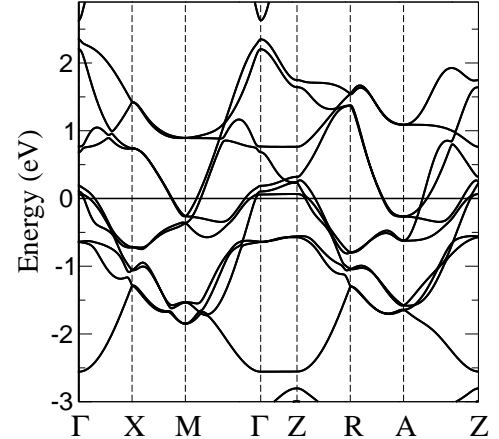


FIG. 3: Band structure of FeSe around the Fermi level (at 0 eV) marked by a horizontal line.

below E_F . It should be noted, that a proximity of the van Hove singularity to the Fermi level is considered as the key ingredient for superconductivity in iron-based superconductors³³.

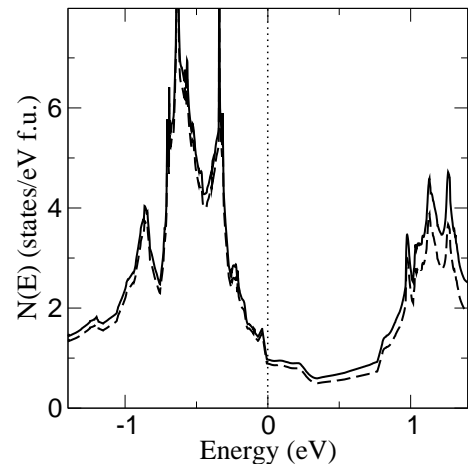


FIG. 4: Total density of electronic states of FeSe (solid line) and the partial contribution of the iron *d*-states (dashed line). The Fermi level position at 0 eV is marked by a vertical line.

To evaluate the paramagnetic susceptibility of FeSe, the FP-LMTO-LSDA calculations of field-induced spin and orbital (Van Vleck) magnetic moments were carried out within the approach described in Ref. 34. The relativistic effects, including spin-orbit coupling, were incorporated, and the effect of an external magnetic field \mathbf{H} was taken into account self-consistently by means of the Zeeman term:

$$\mathcal{H}_Z = \mu_B \mathbf{H} \cdot (2\hat{\mathbf{s}} + \hat{\mathbf{l}}). \quad (1)$$

Here μ_B is the Bohr magneton, $\hat{\mathbf{s}}$ and $\hat{\mathbf{l}}$ are the spin and orbital angular momentum operators, respectively. The

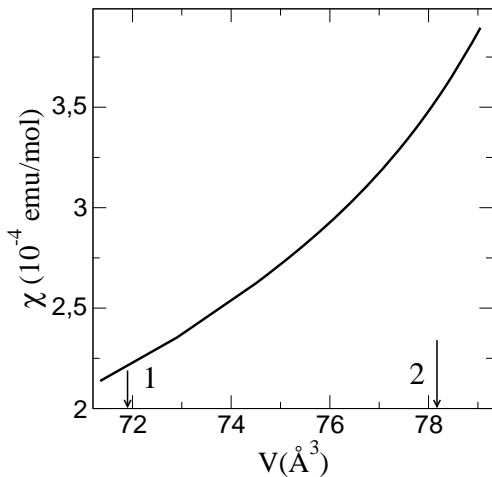


FIG. 5: Calculated paramagnetic susceptibility of FeSe as a function of the unit cell volume (in \AA^3). Z is taken to be 0.26. The arrows indicate the theoretical (1) and experimental (2) equilibrium volume values.

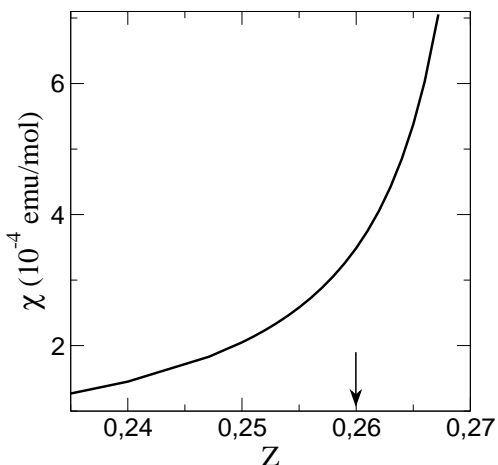


FIG. 6: Calculated paramagnetic susceptibility of FeSe as a function of internal parameter Z for the experimental unit cell volume. The arrow indicates the experimental value of Z .

field induced spin and orbital magnetic moments provide estimations of the related contributions to the magnetic susceptibility, χ_{spin} and χ_{orb} . For the tetragonal crystal structure the components of these contributions, $\chi_{i\parallel}$ and $\chi_{i\perp}$, are derived from the magnetic moments calculated in the external field of 10 T, which was applied parallel and perpendicular to the c axis, respectively.

It is found that magnetic response to the external field is very sensitive to the unit cell volume, as well as to the structural parameter Z , which represents the relative height of chalcogen species from the Fe plane. The calculated dependencies of susceptibility of FeSe as functions of the volume and parameter Z are given in Figs. 5 and 6, respectively.

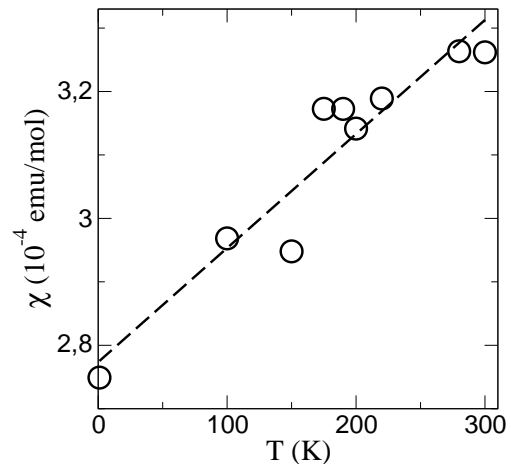


FIG. 7: Calculated temperature dependence of the paramagnetic susceptibility of FeSe. Z is taken to be 0.26, the unit cell volume is fixed between the theoretical and experimental values. The dashed line is a guide for the eye.

Also, the thermal effects are taken into account in order to calculate the temperature dependence of paramagnetic susceptibility for FeSe compound. In this case the field induced spin and orbital magnetic moments were evaluated by corresponding integration with the energy derivative of the Fermi-Dirac distribution function $f(E, \mu, T)$, and the temperature dependence of χ was actually determined by taking into account the finite width of $-df/dE$ (see Ref. 27 for details). It should be noted that the energy derivative of the Fermi-Dirac distribution corresponds to a Dirac delta function at low temperatures, having a sharp positive peak at the Fermi energy E_F . This steep behavior of $-df/dE$ resulted in some instability in the numerical calculations of χ , which are seen in Fig. 7.

IV. DISCUSSION

The experimental superconducting transition temperatures $6\div 8$ K, obtained for the studied FeSe_{1-x} samples, agree with those reported in literature^{1,3-6}. Above T_c , a substantial growth of susceptibility with temperature is revealed in the normal state of FeSe up to 300 K (Fig. 1), what indicates the itinerant nature of electronic states of Fe at the Fermi energy.

The total susceptibility in the absence of spontaneous magnetic ordering can be represented as the sum:

$$\chi_{\text{tot}} = \chi_{\text{spin}} + \chi_{\text{orb}} + \chi_{\text{dia}} + \chi_L, \quad (2)$$

where these terms correspond to the Pauli spin susceptibility, a generalization of the Van Vleck orbital paramagnetism, the Langevin diamagnetism of closed ion shells, and a generalization of Landau conduction electrons diamagnetism, respectively. Obviously, the χ_{dia} term does

not provide any anisotropy, and for FeSe the Langevin diamagnetism of closed ion shells can be estimated according to Ref. 35 as $\chi_{\text{dia}} \simeq -0.2 \times 10^{-4}$ emu/mol.

In order to analyse the experimental data on χ for FeSe we used the calculated paramagnetic contributions to susceptibility, χ_{spin} and χ_{orb} . It has been shown³⁴ that for paramagnetic metallic systems the Stoner approach underestimates the spin susceptibility, whereas the LSDA field-induced calculations take into account non-uniform induced magnetization density in the unit cell and provide more adequate description. The first-principles calculations of the paramagnetic susceptibility for FeSe revealed that this system is in close proximity to the magnetic critical point. This can be seen from a steep rise of $\chi(V)$ and $\chi(Z)$ in Figs. 5 and 6, respectively, above the corresponding experimental values of V and Z . In fact, the calculated Stoner enhancement $S \sim 7$ clearly indicates that FeSe is close to the ferromagnetic Stoner instability.

For the unit cell volume chosen between the theoretical and experimental values, the dominant spin contribution to magnetic susceptibility of FeSe is estimated to be $\chi_{\text{spin}} \simeq 2.4 \times 10^{-4}$ emu/mol. The averaged orbital χ_{orb} term amounts to $\sim 0.4 \times 10^{-4}$ emu/mol, being of about 15% of the total paramagnetism. From comparison of the calculated paramagnetic susceptibility for the ground state in Fig. 7, $\chi_{\text{para}} = \chi_{\text{spin}} + \chi_{\text{orb}} \simeq 2.8 \times 10^{-4}$ emu/mol, with the experimental value χ_{exp} at $T \rightarrow 0$ K in Fig. 1, $\chi_{\text{exp}} = (\chi_{\parallel} + 2\chi_{\perp})/3 \simeq 1.5 \times 10^{-4}$ emu/mol, it is clear that calculated value χ_{para} has to be substantially compensated by a diamagnetic contribution in order to conform with the experimental data. One can estimate the expected diamagnetic contribution to magnetic susceptibility of FeSe to be about $(\chi_{\text{exp}} - \chi_{\text{para}}) \sim -1.3 \times 10^{-4}$ emu/mol. This diamagnetism is comparable in absolute value with the paramagnetic contribution, being much larger than the estimated above Langevin diamagnetism χ_{dia} . Apparently, it can be ascribed to the χ_{L} term in Eq. (2).

According to the experimental data in Fig. 1, the observed anisotropy of susceptibility $\Delta\chi$ is large in FeSe, and even comparable with the averaged susceptibility itself at low temperatures. It appears to be much larger than the calculated anisotropy of orbital contribution to paramagnetic susceptibility of FeSe, $\Delta\chi_{\text{orb}} = \chi_{\text{orb}\parallel} - \chi_{\text{orb}\perp} \simeq -0.1 \times 10^{-4}$ emu/mol. Therefore, in order to explain the experimental $\Delta\chi$ one can assume the presence of a substantial and presumably anisotropic diamagnetic contribution from conduction electrons.

To calculate the Landau diamagnetic contribution χ_{L} is a rather difficult problem^{36,37}. The free-electron Landau approximation, which is often used for estimations, provides χ_{L}^0 that equals $-\frac{1}{3}$ of the Pauli spin susceptibility. However, for many metallic systems the diamagnetism of conduction electrons χ_{L} can be many times larger than the free-electron Landau estimate χ_{L}^0 , and such anomalous and anisotropic diamagnetism is often determined by the presence of quasi-degenerated states

with small effective masses at E_{F} (see Ref. 37 and references therein). As can be seen in Fig. 3, in FeSe the quasi-degenerate states with small effective masses exist at E_{F} around the symmetry points Γ and Z , where the band degeneracies are lifted by the spin-orbital coupling. Such band structure features are of particular importance in connection with a manifestation of the anomalously large and anisotropic χ_{L} , which was found to originate from the similar degeneracy points³⁷. It should be emphasized that rigorous theoretical analysis of χ_{L} is a rather cumbersome procedure, which goes beyond the aims of the present work. At this stage, we have identified appropriate electronic states near E_{F} as possible sources of the large and anisotropic conduction electrons diamagnetism in FeSe.

The theoretically evaluated temperature dependence of the paramagnetic susceptibility $\chi_{\text{para}}(T)$ in Fig. 7, which takes into account the finite width of the energy derivative of the Fermi-Dirac distribution function, actually provides only a slight increase in χ with temperature. Thus, the observed substantial growth of $\chi(T)$ is rather puzzling at present. It is presumably related to a fine structure of DOS at E_{F} , but one should expect that FeSe system is driven far from the ground state at room temperatures. At this stage we should admit that increase of the unit cell volume for the tetragonal $P4/nmm$ phase ($\Delta V/V \simeq 1\%$ with temperature rising up to 300 K, see Ref. 12) can provide about 10% growth of paramagnetic susceptibility, according to the $\chi(V)$ dependence in Fig. 5. However, this volume expansion does not explain the experimental $\chi(T)$ in Fig. 1. Also, a change of the structural parameter Z with temperature can be substantial and of importance due to the strong $\chi(Z)$ dependence in Fig. 6, but to date the influence of temperature on Z was not studied in a systematic way. Therefore, noticeable temperature effects on the lattice parameters, chalcogen atom position Z , and electronic structure itself should be taken into account in a rigorous quantitative analysis of $\chi(T)$ in FeSe.

The measured pressure effects on magnetic susceptibility of FeSe are intriguing and require a detailed examination. Firstly, as can be seen in Table I, there is a striking sign difference for the pressure effects on χ at low and room temperatures. Also, the absolute value of this effect is substantially larger than that observed in strongly enhanced itinerant paramagnets³⁴, and appeared to be comparable with such pressure effect on χ reported for the related FeTe compound²⁴ (see Table I).

It should be noted that the present experimental data on $\chi(T, P)$ for FeSe are in reasonable agreement with the results of Ref. 20 on temperature and pressure dependencies of the NMR Knight shift K of FeSe in the normal state. As can be seen in Fig. 8, the temperature dependence $K(T)$ at ambient pressure reflects the corresponding dependence of the magnetic susceptibility in Fig. 1. Assuming the latter to be governed by the spin susceptibility $\chi_{\text{spin}}(T)$, the only temperature dependent contribution in $K(T)$ can be determined as

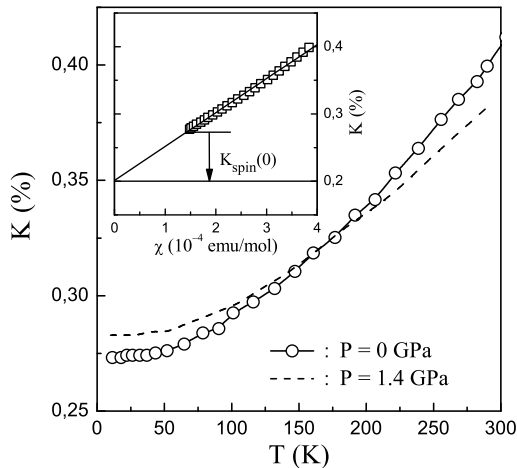


FIG. 8: Temperature dependencies of the NMR Knight shift K in FeSe measured at ambient pressure (\circ) and at $P = 1.4$ GPa (dashed line). The data are taken from Ref. 20. The inset shows dependence of K on the averaged magnetic susceptibility for FeSe, $\chi = (\chi_{\parallel} + 2\chi_{\perp})/3$, from Fig. 1.

$K_{\text{spin}}(T) = \alpha\chi_{\text{spin}}(T)$ with $\alpha \simeq 5 \times 10^2 \text{ \%}(\text{emu/mol})^{-1}$, resulted from the slope of K vs χ linear dependence in inset of Fig. 8. In addition, this contribution is expected to be also responsible for the pressure effect on K . Using a rough approximation $\chi_{\text{spin}}(T) \approx \chi(T)$ we obtain an estimate of $d \ln \chi / dP \approx d \ln K_{\text{spin}} / dP$, which is listed in Table I.

In order to clarify the behavior of $\chi(P)$ in FeSe, we carried out the *ab initio* calculations of paramagnetic sus-

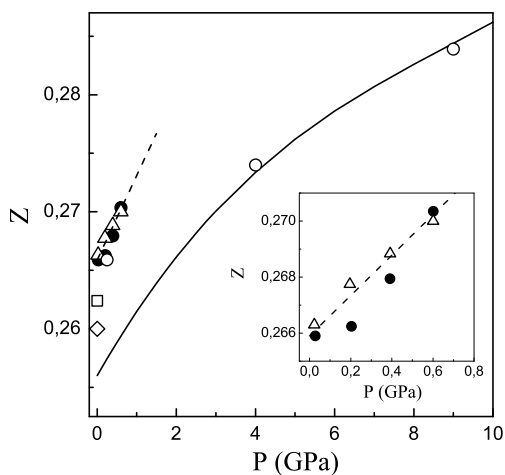


FIG. 9: Pressure dependence of the internal chalcogen structural parameter Z for FeSe. The solid line indicates the results of calculations from Ref. 32. Experimental data on parameter Z in FeSe for the tetragonal phase at $T = 190$ K (Δ , Ref. 7), $T = 295$ K (\square , Ref. 25), $T = 300$ K (\diamond , Ref. 9), and for the orthorhombic phase at $T = 16$ K (\circ , Ref. 3) and $T = 50$ K (\bullet , Ref. 7). In inset: data of Ref. 7 on the expanded scale.

ceptibility as a function of pressure. These calculations are based upon the pressure dependent structural parameters, which have been calculated and listed in Ref. 32. As is seen in Fig. 9, the calculated behavior of $Z(P)$ follows the available experimental data^{3,7,9,14,25}. In the course of corresponding calculations of $\chi(P)$ for FeSe we evaluated the pressure derivative $d \ln \chi / dP \simeq 8 \times 10^{-2} \text{ GPa}^{-1}$ in the range $0 \div 1$ GPa. The evaluated derivative appeared to be in a qualitative agreement with the experimental low temperature data (see Table I).

As part of these electronic structure calculations for FeSe, we also obtained a pressure dependence of the density of states at the Fermi level, which is presented in Fig. 10. In addition to the calculated structural parameters from Ref. 32, we also employed the small upward shift $\Delta Z = +0.004$ to start the optimized $Z(P)$ dependence from the experimental value $Z = 0.26$ (see $Z(P)$ behavior in Fig. 9). The corresponding two sets of calculations demonstrate in Fig. 10 a tolerable variation of $N(E_F)$ behaviors in FeSe under pressure, depending on a small adjustment of $Z(P = 0)$ between the theoretical and experimental values.

With the aim to elucidate the main mechanism of the experimentally observed strong increase of the magnetic susceptibility of FeSe under pressure at low temperatures, we have also analyzed the pressure effect in terms of the corresponding changes of the volume and Z parameters by using the relation:

$$\frac{d \ln \chi}{dP} = \frac{\partial \ln \chi}{\partial \ln V} \times \frac{d \ln V}{dP} + \frac{\partial \ln \chi}{\partial Z} \times \frac{dZ}{dP}. \quad (3)$$

The required values of the partial volume and Z derivatives of χ can be estimated from the results of *ab initio* calculations presented in Figs. 5 and 6, and were found to be $\partial \ln \chi / \partial \ln V \simeq 8$ and $\partial \ln \chi / \partial Z \simeq 65$ for the values of V and Z close to the experimental data. The optimized value $d \ln V / dP = -3 \times 10^{-2} \text{ GPa}^{-1}$ is taken for the compressibility of FeSe³². This calculated compressibility agrees closely with the experimental values $-3.1 \pm 0.1 \times 10^{-2} \text{ GPa}^{-1}$ ^{4,7,13}. Also, the optimized value $dZ/dP \simeq 0.55 \times 10^{-2} \text{ GPa}^{-1}$ was adopted for evaluation of Eq. (3). As is seen in Fig. 9, this value of dZ/dP is in agreement with the experimental data at low pressures. As far as all parameters entering Eq. (3) are estimated, the first term in (3) results in a large negative value $\partial \ln \chi / \partial \ln V \times d \ln V / dP \simeq -24 \times 10^{-2} \text{ GPa}^{-1}$, whereas the second term appears to be large and positive: $\partial \ln \chi / \partial Z \times dZ/dP \simeq 36 \times 10^{-2} \text{ GPa}^{-1}$. The both terms in Eq. (3) taken together yield the estimate $d \ln \chi / dP \simeq 12 \times 10^{-2} \text{ GPa}^{-1}$ for FeSe, which is consistent with the low temperature experimental data. This estimate is also close to the *ab initio* calculated pressure derivative based on theoretical lattice parameters from Ref. 32 ($d \ln \chi / dP \simeq 8 \times 10^{-2} \text{ GPa}^{-1}$, see Table I). Actually, the difference in these evaluated values of $d \ln \chi / dP$, depending on whether experimental or theoretical lattice parameters are employed, covers a reasonable range for the expected pressure effect on χ .

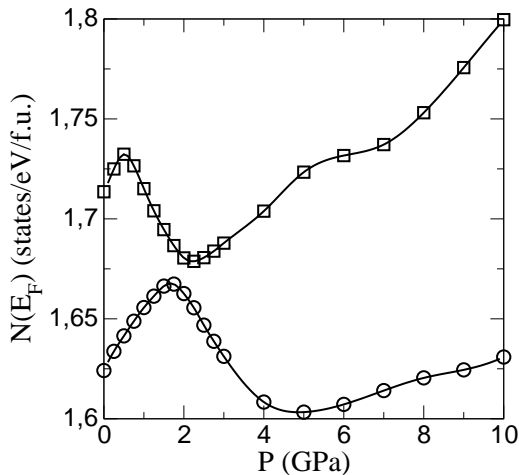


FIG. 10: Calculated pressure dependencies of the density of states at the Fermi level for FeSe. The pressure dependent structural parameters, including the lattice constants and chalcogen atom position Z , were taken from the calculations of Ref. 32 (O). For another set of $N(E_F)$ calculations (\square) the small upward shift $\Delta Z = +0.004$ was employed to start from the experimental value $Z = 0.26$ (see $Z(P)$ behavior in Fig. 9). The solid lines are guides for the eye.

Based on the results of calculations, presented in Figs. 5 and 6, the observed hydrostatic pressure effect on χ in FeSe at low temperatures can be represented as a sum of two large in size and competing contributions, related to the pressure dependence of the structural parameters V and Z . As a result, the experimental positive value of the pressure effect, $d \ln \chi / dP \simeq 10 \times 10^{-2} \text{ GPa}^{-1}$, is determined by a dominating contribution from the change of Z under pressure.

Actually, the nature of the large positive pressure effect on χ in FeSe is similar to that reported for FeTe compound²⁴. However, in the case of FeTe such effect is twice more pronounced, and also takes place at room temperatures, whereas for FeSe $d \ln \chi / dP$ is found to be negative at 300 K (see Table I). The reason of this difference is unclear and have to be elucidated. At the present stage one can presume, that the negative sign of $d \ln \chi / dP$ derivative is probably related to a nature of the observed anomalous growth of $\chi(T)$ up to room temperatures (Fig. 1), which is not the case for FeTe²⁴. It appears that at higher temperatures this anomalous growth of $\chi(T)$ in FeSe is apparently reduced by applied pressure.

Basically, the observed positive pressure effect on χ in FeSe at low temperatures correlates with the calculated increase of the density of states at the Fermi level $N(E_F)$ at low pressures (see Fig. 10). At higher pressures one can see nonmonotonic variation of $N(E_F)$ in Fig. 10 which clearly exhibits consecutive maximum and minimum. It was recently shown³⁸, that superconducting transition temperatures T_c of a number of iron-based superconductors correlate with the corresponding values

of the density of states at the Fermi level, thus supporting the BCS-like pairing mechanism in these systems. Remarkably, that the presently calculated behavior of $N(E_F)$ under pressure (the upper curve in Fig. 10, with maximum at 0.5 GPa and minimum at 2.2 GPa) is qualitatively consistent with the reported experimental dependencies of $T_c(P)$ in FeSe (corresponding maximum and minimum of $T_c(P)$ were observed at $P \simeq 0.8$ GPa and $P \simeq 1.2$ GPa, respectively^{17,18,21,22}). The calculated pressure dependence of DOS at the Fermi level for FeSe with the structural parameters taken from Ref. 32 (the lower curve in Fig. 10) also contains consecutive maximum and minimum of $N(E_F)$, which are substantially shifted to higher pressures.

V. CONCLUSIONS

The magnetic susceptibility of FeSe compound is found to rise substantially with temperature, which apparently points to the itinerant nature of the electronic states of Fe. The calculated paramagnetic susceptibility $\chi_{\text{para}}(T)$ describes qualitatively the experimental dependence $\chi(T)$, however the origin of the observed about twofold increase of χ up to 300 K is puzzling. From comparison of the experimental values of susceptibility and its anisotropy with that calculated for paramagnetic contributions to χ in FeSe, the additional anisotropic diamagnetism is expected to be of the order of -1×10^{-4} emu/mol, which can relate to the diamagnetism of conduction electrons and presumably has its origin in the quasi-degenerate electronic states close to E_F .

The measurements of magnetic susceptibility under hydrostatic pressure revealed a strong positive effect at low temperatures. This effect appeared to be comparable with that reported for the related FeTe compound²⁴, whereas at room temperature the pressure effect for FeSe is found to be also strong, but *negative*.

Our calculations indicate that paramagnetic susceptibility of the FeSe compound is substantially dependent on the unit cell volume V and the relative height Z of Se species above the Fe plane. It is shown that the observed at low temperatures large positive pressure effect on χ is related to the strong sensitivity of the paramagnetic susceptibility to the parameter Z , which determines the dominant positive contribution. The grounds of the negative sign of $d \ln \chi / dP$ derivative in FeSe at 300 K are unclear and probably linked to a nature of the observed anomalous growth of $\chi(T)$. At present one can state that at higher temperatures this anomalous growth of $\chi(T)$ in FeSe is apparently reduced by applied pressure.

The present *ab initio* calculations have demonstrated that for FeSe compound the nonmonotonic behavior of superconducting transition temperature with pressure qualitatively correlates with the density of electronic states at the Fermi level. This indicates a possible realization of the BCS-like pairing mechanism in this system.

Acknowledgments

This work was supported by the Russian-Ukrainian RFBR-NASU project 01-02-12 and 12-02-90405, by Russian Ministry of Science and Education through state

contracts 11.519.11.6012 and 14.740.11.1365, by NASU Young Scientists Grant 03-2012, and by a grant of the President of the Russian Federation for State Support of Young Russian Scientists (MK-1557.2011.5).

-
- * Electronic address: grechnev@ilt.kharkov.ua
- ¹ F. C. Hsu, J. Y. Luo, K. W. Yeh, T. K. Chen, T. W. Huang, P. M. Wu, Y. C. Lee, Y. L. Huang, Y. Y. Chu, D. C. Yan, and M. K. Wu, Proc. Natl. Acad. Sci. U.S.A. **38**, 14262 (2008).
 - ² S. Medvedev, T. M. McQueen, I. A. Troyan, T. Palasyuk, M. I. Erements, R. J. Cava, S. Naghavi, F. Casper, V. Ksenofontov, G. Wortmann, and C. Felser, Nature Materials **8**, 630 (2009).
 - ³ S. Margadonna, Y. Takabayashi, Y. Ohishi, Y. Mizuguchi, Y. Takano, T. Kagayama, T. Nakagawa, M. Takata, and K. Prassides, Phys. Rev. B **80**, 064506 (2009).
 - ⁴ D. Braithwaite, B. Salce, G. Lapertot, F. Bourdarot, C. Marin, D. Aoki, and M. Hanfland, J. Phys. Condens. Matter **21**, 232202 (2009).
 - ⁵ T. M. McQueen, Q. Huang, V. Ksenofontov, C. Felser, Q. Xu, H. Zandbergen, Y. S. Hor, J. Allred, A. J. Williams, D. Qu, J. Checkelsky, N. P. Ong, and R. J. Cava, Phys. Rev. B **79**, 014522 (2009).
 - ⁶ E. Pomjakushina, K. Conder, V. Pomjakushin, M. Bendele, and R. Khasanov, Phys. Rev. B **80**, 024517 (2009).
 - ⁷ J. N. Millican, D. Phelan, E. L. Thomas, J. B. Leao, and E. Carpenter, Solid State Commun. **149**, 707 (2009).
 - ⁸ Y. Mizuguchi and Y. Takano, J. Phys. Soc. Jpn. **79**, 102001 (2010).
 - ⁹ R. Hu, H. Lei, M. Abeykoon, E. S. Bozin, S. J. L. Billinge, J. B. Warren, T. Siegrist, and C. Petrovic, Phys. Rev. B **83**, 224502 (2011).
 - ¹⁰ J.-Y. Lin, Y. S. Hsieh, D. A. Chareev, A. N. Vasiliev, Y. Parsons, and H. D. Yang, Phys. Rev. B **84**, 220507(R) (2011).
 - ¹¹ A. V. Fedorchenko, G. E. Grechnev, V. A. Desnenko, A. S. Panfilov, S. L. Gnatchenko, V. V. Tsurkan, J. Deisenhofer, H.-A. Krug von Nidda, A. Loidl, D. A. Chareev, O. S. Volkova, and A. N. Vasiliev, Fiz. Nizk. Temp. **37**, 100 (2011) [Low Temp. Phys. **37**, 83 (2011)].
 - ¹² Y. Mizuguchi and Y. Takano, Z. Kristallogr. **226**, 417 (2011).
 - ¹³ G. Garbarino, A. Sow, P. Lejay, A. Sulpice, P. Toulemonde, M. Mezouar, and M. Nunez-Regueiro, Europhys. Lett. **86**, 27001 (2009).
 - ¹⁴ R. S. Kumar, Y. Zhang, S. Sinogeikin, Y. Xiao, S. Kumar, P. Chow, A. L. Cornelius, and C. Chen, J. Phys. Chem. B **114**, 12597 (2010).
 - ¹⁵ S. S. Naghavi, S. Chadov, and C. Felser, J. Phys. Condens. Matter **23**, 205601 (2011).
 - ¹⁶ G. Rahman, I. G. Kim, and A. J. Freeman, J. Phys. Condens. Matter **24**, 095502 (2012).
 - ¹⁷ S. Masaki, H. Kotegawa, Y. Hara, K. Murata, Y. Mizuguchi, and Y. Takano, J. Phys. Soc. Jpn. **78**, 063704 (2009).
 - ¹⁸ K. Miyoshi, Y. Takaichi, E. Mutou, K. Fujiwara, and J. Takeuchi, J. Phys. Soc. Jpn. **78**, 093703 (2009).
 - ¹⁹ H. Okabe, N. Takeshita, K. Horigane, T. Muranaka, and J. Akimitsu, Phys. Rev. B **81**, 205119 (2010).
 - ²⁰ T. Imai, K. Ahilan, F. L. Ning, T. M. McQueen, and R. J. Cava, Phys. Rev. Lett. **102**, 177005 (2009).
 - ²¹ M. Bendele, A. Amato, K. Conder, M. Elender, H. Keller, H.-H. Klauss, H. Luetkens, E. Pomjakushina, A. Raselli, and R. Khasanov, Phys. Rev. Lett. **104**, 087003 (2010).
 - ²² M. Bendele, A. Ichsanow, Yu. Pashkevich, L. Keller, Th. Strassle, A. Gusev, E. Pomjakushina, K. Conder, R. Khasanov, and H. Keller, Phys. Rev. B **85**, 064517 (2012).
 - ²³ A. S. Panfilov, Phys. Tech. High Press. **2**, 61 (1992) (in Russian).
 - ²⁴ A. V. Fedorchenko, G. E. Grechnev, V. A. Desnenko, A. S. Panfilov, S. L. Gnatchenko, V. Tsurkan, J. Deisenhofer, A. Loidl, O. S. Volkova, and A. N. Vasiliev, J. Phys. Condens. Matter **23**, 325701 (2011).
 - ²⁵ R. W. Gómez, V. Marquina, J. L. Pérez-Mazariego, R. Escamilla, R. Escudero, M. Quintana, J. J. Hernández-Gómez, R. Ridaura, and M. L. Marquina, J. Supercond. Nov. Magn. **23**, 551 (2010).
 - ²⁶ J. M. Wills, M. Alouani, P. Andersson, A. Delin, O. Eriksson, and A. Grechnev, *Full-Potential Electronic Structure Method: Energy and Force Calculations with Density Functional and Dynamical Mean Field Theory* (Springer, Berlin, 2010).
 - ²⁷ G. E. Grechnev, R. Ahuja, and O. Eriksson, Phys. Rev. B **68** 64414 (2003).
 - ²⁸ U. von Barth and L. Hedin, J. Phys. C: Solid State Phys. **5**, 1629 (1972).
 - ²⁹ A. Subedi, L. Zhang, D. J. Singh, and M.-H. Du, Phys. Rev. B **78**, 134514 (2008).
 - ³⁰ K.-W. Lee, V. Pardo, and W. E. Pickett, Phys. Rev. B **78**, 174502 (2008).
 - ³¹ D. J. Singh, Physica C **469**, 418 (2009).
 - ³² A. Ciechan, M. J. Winiarski, and M. Samsel-Czekala, Acta Phys. Polonica A **121**, 820 (2012).
 - ³³ A. A. Kordyuk, Fiz. Nizk. Temp. **38**, 1119 (2012).
 - ³⁴ G.E. Grechnev, Fiz. Nizk. Temp. **35**, 812 (2009) [Low Temp. Phys. **35** 638 (2009)].
 - ³⁵ P. Selwood, *Magnetochemistry*, (Interscience, N.Y., 1956).
 - ³⁶ G.E. Grechnev, A.V. Fedorchenko, A.V. Logosha, A.S. Panfilov, I.V. Svechkarov, V.B. Filippov, A.B. Lyashchenko, and A.V. Evdokimova, J. Alloys Compd. **481**, 75 (2009).
 - ³⁷ A. E. Baranovskiy, G. E. Grechnev, G. P. Mikitik, and I. V. Svechkarov, Fiz. Nizk. Temp. **29**, 473 (2003) [Low Temp. Phys. **29**, 356 (2003)].
 - ³⁸ M. V. Sadovskii, E. Z. Kuchinskii, and I. A. Nekrasov, J. Magn. Magn. Mater. **324**, 3481 (2012).